Chapter 2
Direct Detection of WIMPs

2.1 Experimental Strategies for WIMP Detection

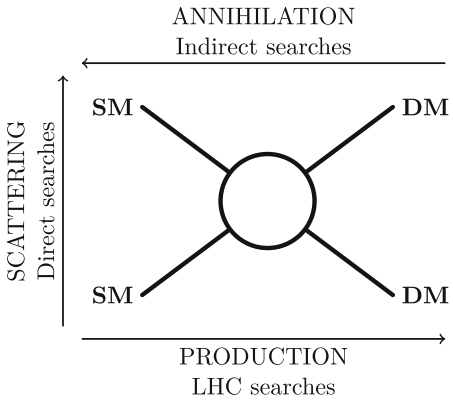
In the next chapters we are going to give an overview of the main WIMP search strategies, which fall in three big categories:

- Direct searches probe the scattering cross section of WIMPs with nuclei, by looking for nuclear recoils in some target material in a low background environment. When a WIMP of the galactic halo passes through the target, it may scatter off a nucleus, whose recoil will be measured by suitable detectors. The main astrophysical uncertainty is due to the DM density in the Solar System and to its velocity distribution.
- Indirect searches look for the products of WIMP annihilations in a number of astrophysical objects, including the galaxy and his satellites, other galaxies and galaxy clusters, as well as the Sun and the Earth.
- In LHC searches, DM particles (and generically the "dark sector") are studied by producing them in proton collisions, in association with other SM particles (being very weakly interacting, WIMPs would otherwise be invisible at colliders, and their typical signature is missing energy in the transverse plane).

© Springer International Publishing AG 2017

E. Morgante, *Aspects of WIMP Dark Matter Searches at Colliders and Other Probes*, Springer Theses, https://doi.org/10.1007/978-3-319-67606-7_2

Pictorially, WIMP searches can be summarized with this diagram:



The simplicity of this representation is somehow misleading. The issue relies in the interpretation of experimental data in terms of a model. In direct searches, the momentum exchange is much lower than the other energy scales which enter the process, and a non-relativistic operators approach is the most suited one. On the contrary, the high energy reach of the LHC requires an interpretation in terms of models whose cut-off is larger than the LHC energy scales (which we will call UV complete models for simplicity), and a less model dependent EFT interpretation is only possible at the price of poorer bounds. It should also be noticed that the physical processes studied in these kind of searches involve very different energy scales, and the effect of running should be taken into account [1].[1] Finally, comparison with indirect searches is also model dependent, and is only meaningful when DM annihilation products include the main proton constituents (light quarks and gluons).

In this chapter we are going to discuss direct searches for WIMPs. The idea dates back to 1984, when Goodman and Witten [2] proposed to try to detect WIMPs by elastic scattering off nuclei in a terrestrial detector. The study was extended by Drukier, Freese and Spergel [3] to include a variety of cold dark matter candidates, as well as details of the detector and the halo model. They also showed that the Earth's motion around the Sun produces an annual modulation in the expected signal. We will start by reviewing the predictions for signal event rates and signatures; then we will turn to briefly discuss the backgrounds, and in particular the so called "neutrino floor"; finally we will describe the current status of direct detection and some of the planned future developments.

[1] The effect is nevertheless minor in the majority of cases, but could become important in view of future precise measurements of DM properties, when (and if) WIMP will ever be discovered.

2.2 Direct Detection: Prediction of Event Rates

Elastic scattering of WIMPs off nuclei has a rate per mass of target material

$$\frac{dR}{dE_R} = \frac{1}{m_{\mathcal{N}}} \frac{\rho_0}{m_\chi} \int_{\mathcal{V}} d^3\vec{v}\, f(\vec{v} + \vec{v}_E)\, v\, \frac{d\sigma}{dE_R}\,, \tag{2.1}$$

where E_R is the nuclear recoil energy, $m_{\mathcal{N}}$ is the mass of the target nuclei, m_χ is the WIMP mass, ρ_0 the local WIMP density in the galactic halo and $d\sigma/dE_R$ is the WIMP-nucleus differential cross section. $\vec{v}$ and $\vec{v}_E$ are the WIMP velocity with respect to the detector and the Earth velocity in the galactic rest frame (which can be assumed to be constant, as far as we are not interested in modulation effects and directional constraints). The function f is the WIMP velocity distribution in the galaxy. The integration domain is defined in such a way that the WIMP velocity with respect to the detector is larger than $v_{\min}$, the minimal velocity of the incoming WIMP in order for the scattering event to be detected. The energy that is transferred to the recoiling nucleus is:

$$E_R = \frac{p^2}{2m_{\mathcal{N}}} = \frac{\mu_{\mathcal{N}}^2 v^2}{m_{\mathcal{N}}}(1 - \cos\theta), \tag{2.2}$$

where p is the momentum transfer, θ is the scattering angle in the WIMP-nucleus centre of mass frame, $m_{\mathcal{N}}$ is the nuclear mass and $\mu_{\mathcal{N}}$ is the WIMP-nucleus reduced mass:

$$\mu_{\mathcal{N}} = \frac{m_{\mathcal{N}} \cdot m_\chi}{m_{\mathcal{N}} + m_\chi}. \tag{2.3}$$

The minimum velocity is given by:

$$v_{\min} = \sqrt{\frac{m_{\mathcal{N}} E_{th}}{2\mu_{\mathcal{N}}^2}}\,, \tag{2.4}$$

where E_{th} is the energy threshold of the detector.

In the simplest galactic model (the so-called standard halo model, which describes an isotropic, isothermal sphere of collisionless particles with density profile $\rho(r) \propto r^{-2}$) the velocity distribution of WIMPs is Maxwellian:

$$f(\vec{v}) = \frac{1}{\sqrt{2\pi}\sigma_v} \exp\left(-\frac{v^2}{2\sigma_v^2}\right). \tag{2.5}$$

The distribution is truncated (and normalized accordingly) at the local escape velocity, which depends on the position in the galaxy, such that $f(\vec{v}) = 0$ for $v \geq v_{\text{esc}}$. The parameters used in the standard halo model are $\rho_0 = 0.3\,\text{GeVcm}^{-3} = 5 \times 10^{-25}\,\text{gcm}^{-3} = 8 \times 10^{-3} M_\odot\,\text{pc}^{-1}$, $v_c = 220\,\text{kms}^{-1}$ and a local escape velocity

of $v_{\rm esc} = 544\,{\rm kms}^{-1}$ (see [4] for a recent discussion on the determination of these parameters and their uncertainties). The underlying assumption is that the phase-space distribution of the dark matter has reached a steady state and is smooth, which may not be the case for the Milky Way, in particular at small scales. Also, it is assumed that no DM disk is present in the Milky Way [5].

A rough numerical estimate of the scattering rate can be easily obtained [5]. Consider a WIMP scattering off a target nucleus, both with mass $\sim 100\,{\rm GeV}$. The mean velocity of the WIMP relative to the target is roughly $\langle v\rangle \sim 220\,{\rm kms}^{-1}$. The mean energy impinged on the nucleus is thus:

$$\langle E_R\rangle = \frac{1}{2} m_\chi \langle v\rangle^2 \sim 30\,{\rm keV}. \tag{2.6}$$

Assuming a local dark matter density of $\rho_0 = 0.3\,{\rm GeVcm}^{-3}$, the number density of WIMPs is $n_0 = \rho_0 m_\chi$, and their flux on Earth is:

$$\phi_0 = n_0 \times \langle v\rangle = \frac{\rho_0}{m_\chi} \times \langle v\rangle = 6.6 \times 10^4\,{\rm cm}^{-2}\,{\rm s}^{-1}. \tag{2.7}$$

An electroweak-scale interaction will have an elastic scattering cross section from the nucleus of $\sigma_{\chi\mathcal{N}} \sim 10^{-38}\,{\rm cm}^2$, leading to a rate for elastic scattering:

$$R \sim 0.1\,\frac{\rm events}{\rm kg\ year}\left[\frac{100}{A} \times \frac{\sigma_{\chi\mathcal{N}}}{10^{-38}\,{\rm cm}^2} \times \frac{\langle v\rangle}{220\,{\rm km\,s}^{-1}} \times \frac{\rho_0}{0.3\,{\rm GeV\,cm}^{-3}}\right]. \tag{2.8}$$

where A is the atomic number of the target nucleus.

2.3 Scattering Cross Section

Being the WIMP velocity of the order of $220\,{\rm kms}^{-1}$, the average momentum transfer may be estimated as

$$\langle p\rangle \simeq \mu_{\mathcal{N}} \langle v\rangle\,, \tag{2.9}$$

which is approximately 6–70 MeV for m_χ between 10 GeV and 1 TeV. The scattering happens then in the extremely non relativistic regime, and will be isotropic in the centre of mass frame. The de Broglie wavelength corresponding to a momentum transfer of $p = 10\,{\rm MeV}/c$ is:

$$\lambda = \frac{h}{p} \simeq 20\,{\rm fm} > r_0 A^{1/3} = 1.25\,{\rm fm}\ A^{1/3}. \tag{2.10}$$

This value is larger than the diameter of most nuclei, and therefore the scattering amplitudes on individual nucleons will, in first approximation, add coherently. Loss

Table 2.1 Non-relativistic operators for WIMP scattering on nuclei

$\mathcal{O}_1 = \mathbb{1}$	$\mathcal{O}_9 = i\vec{S}_\chi \cdot (\vec{S}_N \times \vec{q})$
$\mathcal{O}_2 = (v^\perp)^2$	$\mathcal{O}_{10} = i\vec{S}_N \cdot \vec{q}$
$\mathcal{O}_3 = i\vec{S}_N \cdot (\vec{q} \times \vec{v}^\perp)$	$\mathcal{O}_{11} = i\vec{S}_\chi \cdot \vec{q}$
$\mathcal{O}_4 = \vec{S}_\chi \cdot \vec{S}_N$	$\mathcal{O}_{10}\mathcal{O}_5$
$\mathcal{O}_5 = i\vec{S}_\chi \cdot (\vec{q} \times \vec{v}^\perp)$	$\mathcal{O}_{10}\mathcal{O}_8$
$\mathcal{O}_6 = (\vec{S}_\chi \cdot \vec{q})(\vec{S}_N \cdot \vec{q})$	$\mathcal{O}_{11}\mathcal{O}_3$
$\mathcal{O}_7 = \vec{S}_N \cdot \vec{v}^\perp$	$\mathcal{O}_{11}\mathcal{O}_7$
$\mathcal{O}_8 = \vec{S}_\chi \cdot \vec{v}^\perp$	

of coherence will affect only the tails of velocity distribution, and it is typically parametrized with a nuclear form factor.

The DM-nucleon interaction is determined by a set on non-relativistic operators. The general Lagrangian is

$$\mathcal{L}_{\rm int} = \sum_{N=n,p} \sum_i c_i^{(N)} \mathcal{O}_i \chi^+ \chi^- N^+ N^-, \tag{2.11}$$

where $N^\pm$, $\phi^\pm$ are non-relativistic fields involving only creation or annihilation operators, i.e.

$$N^-(y) \equiv \int \frac{d^3k}{(2\pi)^3} \frac{1}{\sqrt{2m_N}} e^{-ik\cdot y} a_k^\dagger\,, \qquad N^+(y) \equiv (N^-(y))^\dagger\,. \tag{2.12}$$

The list of possible non-relativistic effective operators $\mathcal{O}_i$ is given in Table 2.1 [6] (here we limit ourselves to the operators which can arise from the exchange of spin-0 or spin-1 mediators). Given, in the language of usual relativistic QFT, the Lagrangian that controls the interaction of the WIMP with quarks and gluons, a "dictionary" to translate it into the corresponding non relativistic operators is given in [6, 7].

Generically speaking, operators which are proportional to the velocity of the DM particle or to the exchanged momentum result in a suppressed rate, since both quantities are typically small. In addition, a further suppression is associated to the nucleus spin. A special role in this discussion is played by the operators $\mathcal{O}_1, \mathcal{O}_4$. They arise as the non-relativistic limit of

$$\bar{\chi}\chi\bar{q}q\,,\ \bar{\chi}\gamma_\mu\chi\bar{q}\gamma^\mu q \longrightarrow \mathcal{O}_1\,, \qquad \bar{\chi}\gamma_\mu\gamma_5\chi\bar{q}\gamma^\mu\gamma_5 q \longrightarrow \mathcal{O}_4 \tag{2.13}$$

with appropriate coefficients. They are special in the sense that they are the only operators which are not suppressed by powers of the WIMP velocity or of the momentum transfer. For this reason, they are expected to dominate the scattering cross section, as far as the coefficient in front of the relativistic operator is not vanishing in a specific model (as in the models that will be considered in Chap. 9). These operators are commonly referred to respectively as *spin-independent* and *spin-dependent*, without

further specifications, and limits by experimental collaborations are typically set in terms of the cross section obtained from them.

Assuming that only these two operators are present, the scattering cross section of a WIMP off a nucleus is given by

$$\frac{d\sigma}{dE_R} = \frac{m_{\mathcal{N}}}{2\mu_{\mathcal{N}}^2 v^2}\left[\sigma_{SI} F_{SI}^2(\mathcal{N}, E_R) + \sigma_{SD} F_{SD}^2(\mathcal{N}, E_R)\right], \tag{2.14}$$

where F_{SI} and F_{SD} are the nuclear form factors, that depend on the recoil energy and σ_{SI} and σ_{SD} are the cross sections in the zero momentum transfer limits, which are given by

$$\sigma_{SI} = \frac{4\mu_{\mathcal{N}}^2}{\pi}\left[Z f_p + (A - Z) f_n\right]^2, \tag{2.15}$$

$$\sigma_{SD} = \frac{32\mu_{\mathcal{N}}^2}{\pi} G_F^2 \frac{J+1}{J}\left[a_p \langle S_p\rangle + a_n \langle S_n\rangle\right]^2 . \tag{2.16}$$

Here J the total spin of the nucleus and f_p, f_n and a_p, a_n are the effective WIMP-couplings to neutrons and protons in the spin-independent and spin-dependent case, respectively. These can be calculated using the effective Lagrangian of the given theoretical model. They depend on the contributions of the light quarks to the mass of the nucleons and on the quark spin distribution within the nucleons, respectively, and on the composition of the dark matter particle. The terms in brackets $\langle S_{p,n}\rangle = \langle N|S_{p,n}|N\rangle$ are the expectation values of total proton and neutron spin operators in the limit of zero momentum transfer, and must be determined using detailed nuclear model calculations. We can immediately see that the spin-independent interaction cross section depends on the total number of nucleons, while the spin-dependent cross section is in general smaller, and only relevant for nuclei which have a non-zero spin in their ground state. The reason is that, for the typical DM momenta, its associated de Broglie wavelength is larger than the nuclear size, so the particle interacts coherently with all the nucleus seen as a collection of Z protons and A–Z neutrons. In the spin dependent case this effect does not lead to an enhancement of the cross section because, as it can be understood in terms of the nuclear shell model, nucleons tend to form pairs of zero spin, and the total spin is given only by the unpaired nucleons, whose number is typically not larger than one.

Let us now plug Eq. (2.14) into (2.1). If the scattering is dominated by its spin independent part (which is always the case as soon as a spin independent interaction occurs), and assuming for simplicity that $f_p = f_n$, we obtain

$$\frac{dR}{dE_R} = \frac{\rho_0\, \sigma_{SI}^p}{2\mu_p^2 m_\chi} \times A^2 F_{SI}^2(\mathcal{N}, E_R) \times \mathcal{F}(v_{\min}(m_\chi, E_R, A); \vec{v}_E), \tag{2.17}$$

where we have defined σ_{SI}^p to be the scattering cross section on nucleons, and μ_p the proton-WIMP reduced mass (which for practical purposes can be taken to be equal to the proton mass if the DM is heavier than a few GeV). The factor

$$\mathcal{F} = \int_{\mathcal{V}} \mathrm{d}^3 v \frac{f(\vec{v} + \vec{v}_E)}{v} \tag{2.18}$$

encodes the effect of the DM velocity distribution in the halo, and depends non trivially on m_χ, E_R and $m_\mathcal{N}$ via the minimal velocity $v_{\min}$. Written in this way Eq. (2.17) is very convenient, because it factorises the effect of the DM velocity distribution and the detector related quantities A and F_{SI} (even if, of course, also $\mathcal{F}$ depends on the target material).

Comparing the number of recoil events predicted by means of Eq. (2.17) with data, limits can be derived on σ^p_{SI} (or, analogously, on σ^p_{SD}). Two limits are relevant in order to understand the general feature of the bounds: when the DM particle is very light compared to the target nuclei ($m_\chi \ll m_\mathcal{N}$), the minimal velocity $v_{\min}$ in order for the recoil energy to be detectable becomes very large, and the integration domain of $\mathcal{F}$ closes up. The event rate then goes to zero, and limits get weaker. In order to test lighter and lighter WIMPs, correspondingly light target nuclei are needed. On the other hand, when $m_\chi \gg m_\mathcal{N}$ the minimal velocity does not depend on m_χ any more, and the scattering rate is sensitive to the ratio σ^p_{SI}/m_χ. For this reason, for large mass limits are expected to degrade precisely proportionally to m_χ. The transition between these two regimes lies at $m_\chi \sim m_\mathcal{N}$ (depending also on the threshold), and in this region limits are stronger. In the eventuality of the detection of an excess, in order to disentangle σ^p_{SI} and m_χ it would be necessary to obtain the same measure with different target nuclei [8].

2.4 Backgrounds

The main challenge in direct detection experiments is to reduce the background noise. The first source of background is constituted by environmental radioactivity and cosmic rays (and their secondary products). Environmental radioactivity is faced by shielding the detector and the target material with a combination of different Z materials, with a low intrinsic radioactivity. In particular, the main challenge is provided by neutrons, which can mimic a WIMP signal and constitute an irreducible background, which has to be estimated by means of numerical simulations. The hadronic component of cosmic rays is shielded by the many meters of rock above the detectors which are normally built underground. High energy muons can instead traverse the natural rock shield and produce a flux of energetic neutrons by interacting with nuclei in the rock. These neutrons are in turn slowed down by scattering in the rocks, and may scatter off nuclei in the detector with the typical WIMP energy. In order to reduce these backgrounds a cosmic ray veto is necessary. An additional complication results from the fact that the neutron flux has a seasonal variation which can mimic the WIMP signal modulation. Neutrons from cosmic rays muons will have an increasingly important role in future experiments.

Another threat to background rejection is posed by radioactivity in detector components, both because of radioactive isotopes intrinsically present in the material and because of long lived isotopes produced by cosmic rays during the exposure of the detector and target material at the Earth's surface. This background can only be reduced by appropriate choices of the material and by reducing its exposure time at the Earth's surface.

The most serious issue for future high-sensitivity experiment will be posed by the irreducible neutrino flux, the so-called "ultimate" background. Neutrinos come from a variety of sources. The most relevant for direct detection experiments are neutrinos from fusion reactions in the Sun, decay products of cosmic rays collisions with the atmosphere and relic supernovae neutrinos. Neutrinos coming from radioactive processes on Earth are subdominant [9].

There are two types of neutrino interactions to which dark matter experiments are potentially sensitive: the first is νe^- neutral current elastic scattering, and the second is coherent scattering of neutrinos with target nuclei.

Electron recoils that arise from solar neutrinos from pp reactions have low energies but a very high flux. Depending on the detector capability of discriminate electronic and nuclear recoil, they may become a relevant background at cross sections of 10^{-48} cm^2 or lower [5].

Coherent neutrino-nucleus scattering has never been observed, but it is theoretically a well understood phenomenon. Solar neutrinos (mostly from the decays of ^{8}B and ^{7}Be), atmospheric neutrinos and the ones from the diffuse supernovae background can undergo this kind of scattering. The typical recoil energy is quite low with respect to the one expected by WIMP events, which will make neutrino background even more problematic for future low threshold experiments. An indication of the importance of this background is given in [10]. In this paper, the effect of increased exposure is considered and it was shown that limits can not be pushed below a certain threshold, depending on the DM mass. For a DM particle of mass 10 GeV–10 TeV, the limit is at the level of 10^{-49}–10^{-48} cm^2, not far from the reach of next generation experiments (as we will discuss in Sect. 2.6).

Strictly speaking, a discovery limit exists only if the spectrum of nuclear recoil from WIMPs and from neutrinos coincide. This is the case, for example, of a 6 GeV DM particle with the background of ^{8}B neutrinos in a Xenon detector [10]. Otherwise, a precise determination of the energy spectrum of the events will help in discriminating between the two sources, together with the use of different target sources.

The other two tools that will help in discriminating the neutrino background are seasonal modulation and directional detection, which will be useful especially for light WIMP searches (since for heavy particles their kinetic energy may be large even if the WIMP velocity is directed parallel to the Earth's motion, resulting in a lower relative speed). The effect of directional detectors is carefully computed in [11]. Notice that the detection of neutrino scattering in next generation direct detection experiments can be also seen as a useful tool in order to precisely measure solar neutrino fluxes and test our knowledge of solar physics and of the Standard Model as well [12].

2.5 Specific WIMP Signatures

In order to detect a WIMP-induced signal in direct detection experiments, a specific signature unambiguously pointing towards a galactic halo particle would be needed. This signature might be provided by the Earth's motion around the Sun, which induces a seasonal modulation of the total event rate [3, 13]. The modulation has a purely kinematic origin. The Earth's velocity in the galactic rest frame is a superposition of the Earth's rotation around the Sun and the Sun's rotation around the galactic centre. As a consequence of this, the velocity distribution of the DM particles as viewed from Earth varies with a period of 1 year. The Earth's orbital speed is much smaller than the Sun's one, and therefore the seasonal variation is a small effect that can be parametrized as

$$\frac{\mathrm{d}R}{\mathrm{d}E_R}(E_R, t) \simeq \frac{\mathrm{d}R}{\mathrm{d}E_R}(E_R)\left[1 + \Delta(E_R)\cos\frac{2\pi\,(t - t_0)}{T}\right] \tag{2.19}$$

where, under the simplifying assumption that the DM velocity distribution in the galaxy is isotropic, $T = 1$ year and the phase is $t_0 = 150$ days [5]. The amplitude of the modulation $\Delta(E_R)$ becomes negative at small recoil energies, meaning that the differential event rates peaks in winter for small recoil energies, and in summer for larger recoils energies.

Seasonal modulated phenomena are unfortunately ubiquitous on Earth, and therefore many effects can mimic a WIMP signal. For this reason, directional signatures would highly improve the discrimination capability of direct search experiments [14, 15]. In particular, since the WIMP flux in the lab frame is peaked in the direction of motion of the Sun, namely towards the constellation Cygnus, the recoil spectrum is peaked in the opposite direction, leading to a very large forward-backward asymmetry of order $\mathcal{O}(v_\odot/\langle v\rangle) \approx 1$. Thus fewer events, namely a few tens to a few hundreds, depending on the halo model, are needed to discover a WIMP signal compared to the case where the seasonal modulation effect is exploited [15, 16]. The experimental challenge is to build massive detectors capable of detecting the direction of the incoming WIMP.

2.6 Present Status and Future Development

Present upper limits and future prospects on the spin independent WIMP-nucleon cross section are presented in Fig. 2.1. A large variety of techniques are employed in direct WIMP searches. Heat deposition, ionization, and scintillation are used in order to detect the recoil energy in a number of different materials. In the low WIMP mass region (roughly below 6 GeV) cryogenic detectors with a very low energy threshold and light target nuclei perform the best. Currently, the best limits come from the DAMIC [29], CRESST [18, 30], EDELWEISS [31] and SuperCDMS [19, 32] experiments, as well as the liquid Xenon experiments LUX [33] and XENON100 [34]. For

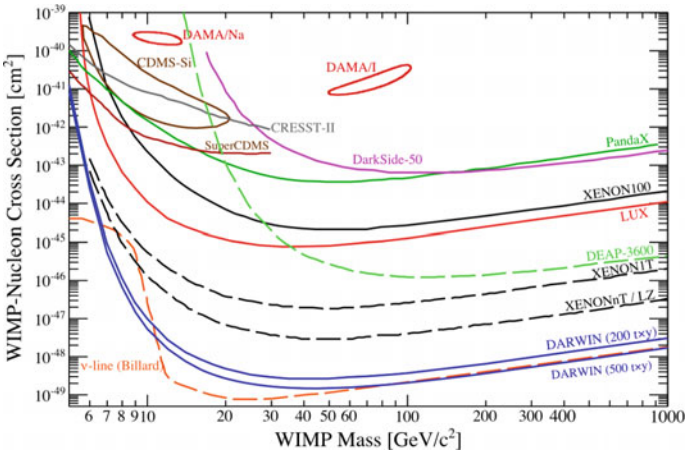


Fig. 2.1 Collection of bounds on σ_{SI}, from [17]. Upper limits are shown from CRESST-II [18], SuperCDMS [19], Panda-X [20], XENON-100 [21] and LUX [22], together with projections for DEAP-3600 [23], XENON1T [24], XENONnT [25], LZ [26] and DARWIN [27]. Updated results from LUX [28] improve current best upper limits by roughly a factor of 4 in the region $m_\chi \gtrsim 100\,\mathrm{GeV}$

larger WIMP masses, liquid Xenon experiments are able to place stronger bounds. The stronger ones come from the LUX experiment [22, 28, 33, 35], improving upon previous bounds from XENON100 [21].

When spin dependent interactions are considered, nuclei with a non-zero intrinsic angular momentum are needed. A particularly suitable one is ^{19}F, which is part of the target material of experiments as PICASSO [36], COUPP [37], SIMPLE [38] and PICO-2L [39]. The most stringent bounds for large DM mass come from the PICO-2L and LUX experiments, while for light DM PICASSO is stronger. The light spin 1/2 nucleus ^{3}He could also be used for spin dependent WIMP interactions. The advantage is that it is technologically feasible to obtain large amounts of highly polarized material, which would help in rejecting the solar neutrino background [40], since the polarization modulated amplitude is large for neutrino-nucleus scattering (and can therefore cancel the polarization independent part if the polarization direction is chosen properly with respect to the direction of arrival from the Sun) but small for WIMPS due to velocity suppression.

In the past years, several anomalies were observed and later understood as due to background processes, in particular in the low WIMP mass region (as the one claimed by the CoGeNT experiment). Only two of them remain unexplained, by the CDMS-Si [41] and the DAMA/LIBRA [42, 43] experiments. The former have seen an excess of events over a very low background. The latter reports an annual variation of single-scatter event rate at low energy, compatible with WIMP interpretation. In both cases the relevant region in parameter space has been excluded by other searches, and the situation is still far from being clear. It can surely be said that, up to now, no settled WIMP signal has been seen by direct detection experiments.

Several new experiments are in data-taking, commissioning or planning phase, aiming towards improving the constrain capability both in the low and high WIMP mass region. Among them it is worth remember DEAP-3600 [23], XENON1T [24], XENONnT [25], LZ [26, 44] and DARWIN [27]. The latter, which will operate multi-tons of target material, will probably be the first experiment able to reach the region where the neutrino background becomes visible. To go beyond this point several technological advances will be needed. Directional detectors will probably be the next stage.

A complementary direction to the one of enlarging experiments is that of lowering the threshold by considering events different from nuclear recoils, in order to improve the exclusion potential for DM masses in the range keV-GeV. These include electronic recoils from ionization events [45–47], electronic excitation and de-excitation with the consequent photon emission [45, 48], molecular dissociation with the production of ions, and finally phonon or heat production [45], electron scattering in semiconductor materials [47, 49, 50], in superfluids [51, 52] and in superconductors [53, 54], exploiting bremsstrahlung in low recoil energy nuclear scatterings [55] or the high velocity of DM particles from evaporation in the Sun (a phenomenon which we will describe in details in Chap. 3) [56]. Interestingly, searches in the low mass range could have directional sensitivity if performed with 2D graphene targets, as recently proposed in [57]. The information on the incoming direction of the DM particle is retained by scattered electrons, and it is not lost in further electrons' scatterings inside the bulk material.

It should anyway be noticed that this discussion assumed that the interaction of the DM with target nuclei is spin independent. When the interaction is mediated by an operator different from $\mathcal{O}_1$ in Table 2.1 (*i.e.* when it is spin and/or velocity dependent) constraints are much weaker, and the neutrino background is not a concern. Models in which the spin independent part of the interaction is absent are non generic, but have very interesting phenomenology as we will discuss in the example of Chap. 9.

References

1. F. D'Eramo, B.J. Kavanagh, P. Panci, You can hide but you have to run: direct detection with vector mediators, JHEP **1608** (2016) 11, arXiv:1605.04917
2. M.W. Goodman, E. Witten, Detectability of certain dark matter candidates. Phys. Rev. D **31**, 3059 (1985)
3. A.K. Drukier, K. Freese, D.N. Spergel, Detecting cold dark matter candidates. Phys. Rev. D **33**, 3495–3508 (1986)
4. A.M. Green, Astrophysical uncertainties on direct detection experiments, Mod. Phys. Lett. A **27**, 1230004 (2012), arXiv:1112.0524
5. L. Baudis, Direct dark matter detection: the next decade, Phys. Dark Univ. **1**, 94–108 (2012) arXiv:1211.7222
6. A.L. Fitzpatrick, W. Haxton, E. Katz, N. Lubbers, Y. Xu, The effective field theory of dark matter direct detection, JCAP **1302** 004 (2013), arXiv:1203.3542
7. M. Cirelli, E. Del Nobile, P. Panci, Tools for model-independent bounds in direct dark matter searches, JCAP **1310**(019), (2013), arXiv:1307.5955

8. M. Pato, L. Baudis, G. Bertone, R.R. de Austri, L.E. Strigari, R. Trotta, Complementarity of dark matter direct detection targets, Phys. Rev. D **83** 083505, (2011), arXiv:1012.3458
9. J. Monroe, P. Fisher, Neutrino backgrounds to dark matter searches, Phys. Rev. D **76**, 033007 (2007), arXiv:0706.3019
10. J. Billard, L. Strigari, E. Figueroa-Feliciano, Implication of neutrino backgrounds on the reach of next generation dark matter direct detection experiments, Phys. Rev. D **89**(2), 023524 (2014), arXiv:1307.5458
11. P. Grothaus, M. Fairbairn, J. Monroe, Directional dark matter detection beyond the neutrino bound, Phys. Rev. D **90**(5), 055018 (2014), arXiv:1406.5047
12. D.G. Cerdeño, M. Fairbairn, T. Jubb, P.A.N. Machado, A.C. Vincent, and C. Bœhm, Physics from solar neutrinos in dark matter direct detection experiments, JHEP **05** 118, (2016), arXiv:1604.01025
13. K. Freese, J.A. Frieman, A. Gould, Signal modulation in cold dark matter detection. Phys. Rev. D **37**, 3388–3405 (1988)
14. D.N. Spergel, The motion of the earth and the detection of wimps. Phys. Rev. D **37**, 1353 (1988)
15. C.J. Copi, J. Heo, and L.M. Krauss, Directional sensitivity, WIMP detection, and the galactic halo, Phys. Lett. B **461** 43–48 (1999), arXiv:hep-ph/9904499
16. C.J. Copi L.M. Krauss, Angular signatures for galactic halo WIMP scattering in direct detectors: prospects and challenges, Phys. Rev. D **63**, 043507 (2001), arXiv:astro-ph/0009467
17. L. Baudis, Dark matter detection. J. Phys. G **43**(4), 044001 (2016)
18. CRESST-II Collaboration, G. Angloher et al., Results on low mass WIMPs using an upgraded CRESST-II detector, Eur. Phys. J. C **74**(12), 3184 (2014), arXiv:1407.3146
19. SuperCDMS Collaboration, R. Agnese et al., Search for low-mass weakly interacting massive particles with SuperCDMS, Phys. Rev. Lett. **112**(24), 241302 (2014), arXiv:1402.7137
20. PandaX Collaboration, M. Xiao et al., First dark matter search results from the PandaX-I experiment, Sci. China Phys. Mech. Astron. **57**, 2024–2030 (2014), arXiv:1408.5114
21. XENON100 Collaboration, E. Aprile et al., Dark matter results from 225 live days of XENON100 data, Phys. Rev. Lett. **109**, 181301 (2012), arXiv:1207.5988
22. LUX Collaboration, D.S. Akerib et al., First results from the LUX dark matter experiment at the Sanford underground research facility, Phys. Rev. Lett. **112**, 091303 (2014), arXiv:1310.8214
23. DEAP Collaboration, M.G. Boulay, DEAP-3600 dark matter search at SNOLAB, J. Phys. Conf. Ser. **375** 012027 (2012), arXiv:1203.0604
24. XENON1T Collaboration, E. Aprile, The XENON1T dark matter search experiment, Springer Proc. Phys. **148** 93–96 (2013), arXiv:1206.6288
25. XENON1T Collaboration, E. Aprile et al., Conceptual design and simulation of a water Cherenkov muon veto for the XENON1T experiment, JINST **9** 11006 (2014), arXiv:1406.2374
26. D.C. Malling et al., After LUX: the LZ program, arXiv:1110.0103
27. DARWIN Consortium Collaboration, L. Baudis, DARWIN: dark matter WIMP search with noble liquids, J. Phys. Conf. Ser. **375** 012028 (2012), arXiv:1201.2402
28. A. Manalaysay, L.U.X. the dark matter search, *Talk at IDM2016* (Sheffield, UK, 2016)
29. DAMIC Collaboration, J.R.T. de Mello Neto et al., The DAMIC dark matter experiment, in Proceedings, 34th International Cosmic Ray Conference (ICRC 2015), (2015), arXiv:1510.02126
30. CRESST Collaboration, G. Angloher et al., Results on light dark matter particles with a low-threshold CRESST-II detector, Eur. Phys. J. C 76(1), 25 (2016), arXiv:1509.01515
31. EDELWEISS Collaboration, E. Armengaud et al., Constraints on low-mass WIMPs from the EDELWEISS-III dark matter search, JCAP **1605**(5), 019 (2016), arXiv:1603.05120
32. SuperCDMS Collaboration, R. Agnese et al., New results from the search for low-mass weakly interacting massive particles with the CDMS low ionization threshold experiment, Phys. Rev. Lett. **116**(7), 071301 (2016), arXiv:1509.02448
33. LUX Collaboration, D. S. Akerib et al., Improved limits on scattering of weakly interacting massive particles from reanalysis of 2013 LUX data, Phys. Rev. Lett. **116**(16), 161301 (2016), arXiv:1512.03506

34. XENON100 Collaboration, E. Aprile et al., A low-mass dark matter search using ionization signals in XENON100, arXiv:1605.06262
35. LUX Collaboration, D.S. Akerib et al., The large underground xenon (LUX) Experiment, Nucl. Instrum. Meth. A **704**, 111–126 (2013), arXiv:1211.3788
36. PICASSO Collaboration, S. Archambault et al., Constraints on low-mass WIMP interactions on ^{19}F from PICASSO, Phys. Lett. B **711**, 153–161 (2012), arXiv:1202.1240
37. COUPP Collaboration, E. Behnke et al., First dark matter search results from a 4-kg CF_3I bubble chamber operated in a deep underground site, Phys. Rev. D **86**(5), 052001 (2012), arXiv:1204.3094. [Erratum: Phys. Rev.D90,no.7,079902(2014)]
38. M. Felizardo et al., Final analysis and results of the phase II simple dark matter search, Phys. Rev. Lett. **108**, 201302 (2012), arXiv:1106.3014
39. PICO Collaboration, C. Amole et al., Dark matter search results from the PICO-2L C_3F_8 bubble chamber, Phys. Rev. Lett. **114**(23), 231302 (2015), arXiv:1503.00008
40. T. Franarin, M. Fairbairn, Reducing the solar neutrino background using polarised Helium-3, Phys. Rev. D 94(5), 053004 (2016), arXiv:1605.08727
41. CDMS Collaboration, R. Agnese et al., Silicon detector dark matter results from the final exposure of CDMS II, Phys. Rev. Lett. **111**(25), 251301 (2013), arXiv:1304.4279
42. DAMA Collaboration, R. Bernabei et al., First results from DAMA/LIBRA and the combined results with DAMA/NaI, Eur. Phys. J. C **C56**, 333–355 (2008), arXiv:0804.2741
43. DAMA, LIBRA Collaboration, R. Bernabei et al., New results from DAMA/LIBRA, Eur. Phys. J. C **67**, 39–49 (2010), arXiv:1002.1028
44. LZ Collaboration, D.S. Akerib et al., LUX-ZEPLIN (LZ) Conceptual Design Report, arXiv:1509.02910
45. R. Essig, J. Mardon, T. Volansky, Direct detection of sub-GeV dark matter, Phys. Rev. D **85** 076007 (2012), arXiv:1108.5383
46. R. Essig, A. Manalaysay, J. Mardon, P. Sorensen, T. Volansky, First direct detection limits on sub-GeV dark matter from XENON10, Phys. Rev. Lett. **109**, 021301 (2012), arXiv:1206.2644
47. S.K. Lee, M. Lisanti, S. Mishra-Sharma, and B.R. Safdi, Modulation effects in dark matter-electron scattering experiments, Phys. Rev. D **92**(8), 083517 (2015), arXiv:1508.07361
48. S. Derenzo, R. Essig, A. Massari, A. Soto, T.-T. Yu, Direct detection of sub-gev dark matter with scintillating targets, Phys. Rev. D 96(1), 016026 (2017), arXiv:1607.01009
49. P.W. Graham, D.E. Kaplan, S. Rajendran, M.T. Walters, Semiconductor probes of light dark matter, Phys. Dark Univ. **1**, 32–49 (2012), arXiv:1203.2531
50. R. Essig, M. Fernandez-Serra, J. Mardon, A. Soto, T. Volansky, T.-T. Yu, Direct detection of sub-GeV dark matter with semiconductor targets, JHEP **05**, 046 (2016), arXiv:1509.01598
51. W. Guo, D.N. McKinsey, Concept for a dark matter detector using liquid helium-4, Phys. Rev. D **87**(11), 115001 (2013), arXiv:1302.0534
52. K. Schutz, K.M. Zurek, On the detectability of light dark matter with superfluid Helium, Phys. Rev. Lett. 117(12), 121302 (2016), arXiv:1604.08206
53. Y. Hochberg, Y. Zhao, K.M. Zurek, Superconducting detectors for superlight dark matter, Phys. Rev. Lett. **116**(1), 011301 (2016), arXiv:1504.07237
54. Y. Hochberg, M. Pyle, Y. Zhao, K.M. Zurek, Detecting superlight dark matter with fermi-degenerate materials, JHEP **1608**, 057 (2016), arXiv:1512.04533
55. C. Kouvaris, J. Pradler, Probing sub-GeV dark matter with conventional detectors, Phys. Rev. Lett. **118**(3), 031803 (2017), arXiv:1607.01789
56. C. Kouvaris, Probing light dark matter via evaporation from the sun, Phys. Rev. D **92**(7), 075001 (2015), arXiv:1506.04316
57. Y. Hochberg, Y. Kahn, M. Lisanti, C.G. Tully, K.M. Zurek, Directional detection of dark matter with 2D targets, Phys. Lett. B772, 239–246, (2017), arXiv:1606.08849



http://www.springer.com/978-3-319-67605-0

Aspects of WIMP Dark Matter Searches at Colliders and Other Probes

Morgante, E.

2017, XX, 212 p. 50 illus., 42 illus. in color., Hardcover
ISBN: 978-3-319-67605-0